6th European Conference on Computational Mechanics (ECCM 6)
7th European Conference on Computational Fluid Dynamics (ECFD 7)
11 – 15 June 2018, Glasgow, UK

DEVELOPMENT OF SIMULATION METHOD FOR CRACK PROPAGATION AND CORROSION PRODUCT MOVEMENT DUE TO REBAR CORROSION

HIKARU NAKAMURA[1], ZAHRA AMALIA[2] DI QIAO[3] AND TAITO MIURA[3]

[1]Nagoya University
Furo-cho, Chikusa-ku, Nagoya, 464-8603, JAPAN
hikaru@nagoya-u.jp, http://concrete-lab.civil.nagoya-u.ac.jp/homepage/j/en/index.html

[2]Nagoya University
Furo-cho, Chikusa-ku, Nagoya, 464-8603, JAPAN
zahra.amalia96@gmail.com

[3]Takenaka Research & Development Institute
1-5-1 Ohtsuka, Inzai-shi, Chiba, 270-1395, JAPAN
qiao.di@takenaka.co.jp

[4]Nagoya University
Furo-cho Chikusa-ku Nagoya, 464-8603, JAPAN
t.miura@civil.nagoya-u.ac.jp

Key words: Corrosion, RBSM, Truss-Network, Crack Propagation, Diffusion.

Abstract. In this paper, both experimental and numerical studies were carried out to evaluate concrete cracking behavior and corrosion products movement during rebar corrosion process. The electric corrosion tests with an applied current density of 900μA/cm^2 were conducted, in which the development of surface and internal cracks was investigated. Considering test results, a numerical model based on three-dimensional Rigid Body Spring Method combined with Truss Network model was developed, which treated the corrosion products movement as a diffusion problem. The model was validated against the test results, showing that it can reasonably reproduce the effect of corrosion products movement on the crack propagation.

1 INTRODUCTION

The development of corrosion-caused cracks is affected by material properties of the corrosion products, such as the expansion ratio, stiffness, and their transport properties. There are several test results suggesting that part of corrosion products may penetrate to the concrete pores and cracks, which do not contribute to the expansion pressure[1]. Their study indicate that the movement of corrosion products may affect the crack initiation process and crack propagation due to the reduction of expansion pressure, thus it should be considered as a concept for modeling the cracking process.

Such experimental observation has been considered in several numerical models developed for evaluating corrosion-induced cracking process. For predicting the time to crack initiation,

some researchers assumed that there was a porous zone with a specific thickness around the steel bar, and the corrosion products firstly filled this zone before generating any expansion pressure[2][3]. On the other hand, some adopted the calibrated expansion ratio and/or stiffness in their models[4][5], which were substantially smaller than those found in the tests[6][7]. For simulating the crack propagation, the amount of the corrosion products that effectively contribute to concrete cracking was often decided with consideration of the crack volume, into which the corrosion products can be accommodated[4][8]. Although these modeling techniques can simulate the effect of corrosion products movement on the crack development indirectly, the applied parameters may vary significantly depends on the model. A more sophisticated model describing the corrosion products movement as a convective-diffusion problem was reported by Ožbolt et al.[9]. This model, however, was not confirmed with any test results, and the parameters influencing such a problem were still unclear.

The aim of this paper is to develop a model of corrosion-induced crack width accurately by considering the corrosion products movement in a quantitative manner. A numerical model considering the moving process as a diffusion problem is developed using the Rigid Body Spring Method (RBSM) and the Truss Network model, in which the crack aided moving process is highlighted. The model is validated by comparing with the test results in terms of crack width and pattern. In addition, the parameters that play a key role in the moving process are investigated.

2 EXPERIMENTAL STUDY

The experimental study was conducted to obtain essential data for the modeling validation, in which accelerated electric corrosion tests were carried out and the surface crack propagation was continuously recorded with strain gauge typed displacement transducers.

2.1 Test procedure

The test specimens had a dimension of 150×150×300mm^3 with a cast-in deformed rebar, which was 250mm long, and the concrete cover was 30mm. Figure 1 shows the specimen geometry. The nominal diameter of the rebar was 19mm. Six specimens were cast and corroded to obtain various surface crack widths. The concrete was made using early strength Portland cement. The maximum diameter of the coarse aggregates was 20mm. After casting, the specimens were cured under sealed conditions in a curing room at 20°C for 14days. Before starting the corrosion test, compressive and splitting tensile tests were conducted using cylinder specimens. The elastic modulus, compressive strength, and splitting tensile strength were decided as 27.62GPa, 37.25MPa, and 2.70MPa, respectively.

To accelerate the corrosion process, each specimen was partly immersed in a pool filled with 3% NaCl solution, which acted as an electrolyte to provide Cl- ions in the electric corrosion test. A copper plate served as the cathode was immersed in the NaCl solution and connected to a direct current (DC) power source together with the rebar, which was the anode. During the test, the current density was kept as constant as 900μA/cm^2. To record the surface crack propagation, two displacement transducers were mounted on the top surface as shown in Figure1. This test method was used in our previous study[8]. The corrosion test time was varied to reach a range of surface crack widths.

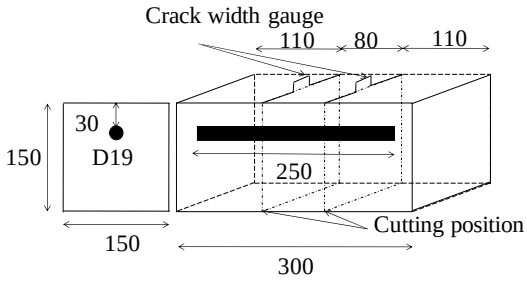

Figure 1: Specimen geometry (unit: mm)

When the corrosion tests reached each designed surface crack width, the specimen was cut along two sections as shown in Figure1 to examine the internal crack patterns. The corroded rebar segments were then taken out and immersed in a 10% ammonium citrate solution for 24 hours to remove the corrosion products. Their weights were measured, and the corrosion amount was calculated by dividing the mass loss by the wet surface area.

2.2 Internal and surface crack development

During the test, a single surface crack was found along the length direction of the rebar. Figure 2 shows the development of internal cracks. Initially, a vertical crack was observed near the top surface of the specimen. As the corrosion amount increased, this crack propagated towards the rebar and two lateral cracks also developed.

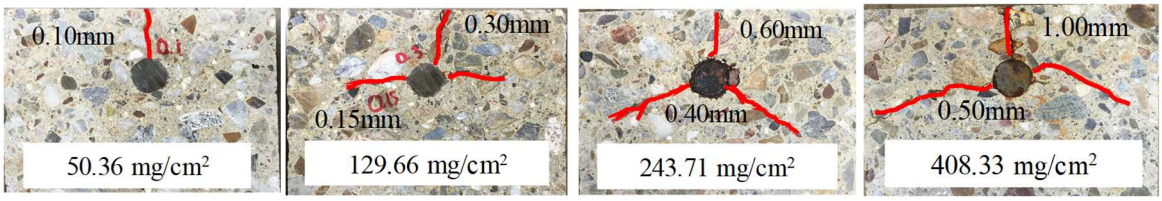

(a) 0.15mm (b) 0.67mm (c) 0.36mm (d) 1.15mm

Figure 2: Development of internal cracks at different surface crack width

To clarify the time-dependent surface cracking behavior, the relationship between corrosion amount and current flow was derived as shown in Figure 3. A bilinear relationship was found to best fit the test data. At the early stage, the actual corrosion amount was lower than the theoretical one predicted by Faraday's law with assumed full current efficiency (N=1). As the corrosion continued and the surface crack width developed, the current efficiency increased with a higher slope. These results showed the same behavior as obtained in the results of Tran et al.[8]. Based on Figure 3, the empirical equations for deciding the real-time corrosion amount are presented as follows [8]:

$$Wr = 0.00079It, \quad It < 66A*hr \qquad (1)$$
$$= 0.0021It-0.085, \quad It > 66A*hr$$

where I and t are the applied electric current intensity (A) and the testing time (hour), respectively.

Figure 4 shows the development of surface crack width against the corrosion amount. For the crack initiation, the critical corrosion amount was around 25mg/cm^2. On the other hand, the crack propagation was found to become slower when the crack width was larger than

0.4mm, showing a two-stage bilinear process. A similar behavior has been observed by Pedrosa and Andrade[10]. This reduction could be ascribed to the decrease of expansion pressure resulting from the corrosion products movement.

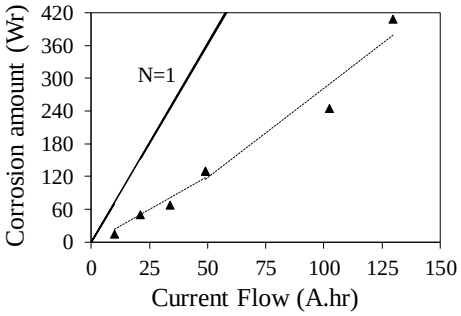

Figure3: Relationship between current flow and corrosion amount

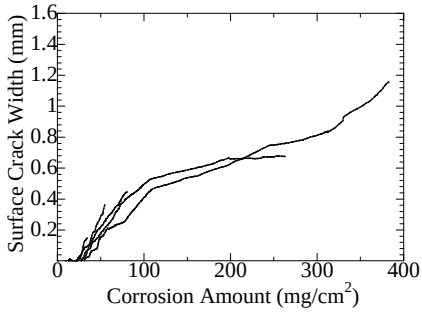

Figure4: Development of surface crack width

3 DEVELOPMENT OF SIMULATION METHOD

3.1 Three-dimensional RBSM

RBSM is one of the discrete numerical approaches, which represents a continuum material as an assemblage of rigid particles interconnected by zero-length springs along their boundaries as shown in Figure 5. The Voronoi diagram is used to randomly generate the particle elements, which have six degrees of freedom at each center point. The boundary between each two adjacent elements is divided into triangles that are formed by the center of gravity and vertices of the boundary. There are three springs set at the center of each formed triangle, two shear springs and one normal spring. The springs are applied with nonlinear material models of concrete. The advantage of this method is that crack widths can be easily measured during the analysis.

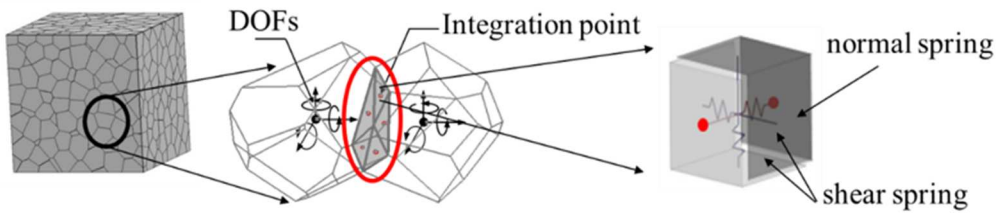

Figure 5: Rigid Body Spring Method

In this analysis, three-dimensional RBSM was used[11][12]. The concrete material model applied in this analysis is shown in Figure 6. The tensile and compressive models were introduced into the normal springs. In these models, f_t stands for tensile strength, h is the distance between centers of the elements, G_F is tensile fracture energy, f_c' is compressive strength, G_{Fc} is compressive fracture energy and E is Young modulus. A linear behavior of tension was modeled up to the tensile strength, and after cracking a bilinear softening behavior was assumed as shown in Figure 6(a). For the compressive model, the hardening behavior up to compressive strength was modeled by using a parabolic curve, while a linear softening was assumed after the peak stress. The shear model was introduced into the shear springs as shown in Figure 6(b). The shear strength was assumed to follow the Mohr-

Coulomb type criterion with the tension and compression caps. Furthermore, at the cracked interface, the shear transferring ability changed based on the crack opening. Thus, the shear stiffness G was reduced by using a function of the strain normal to the crack as shown in the shear reduction model. The material parameters of concrete were decided by performing a compression analysis of a standard cylinder, which was compared with the test data.

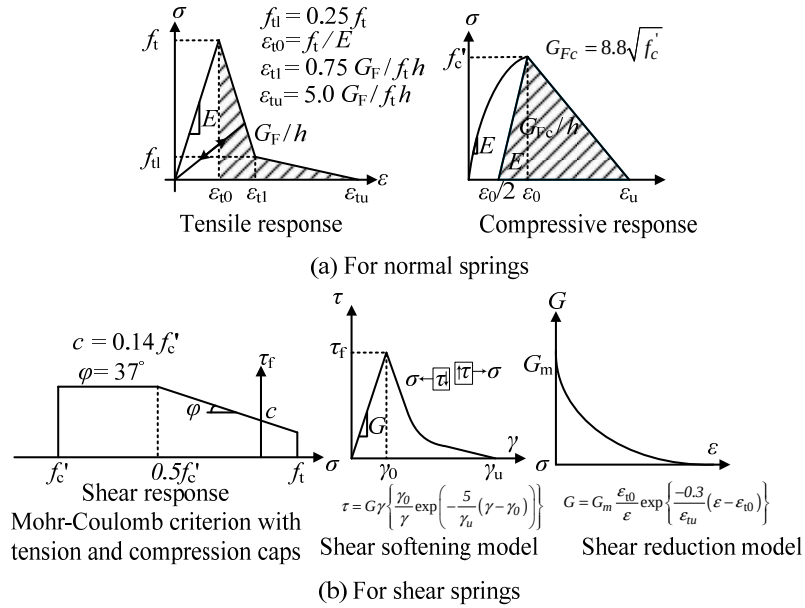

Figure 6: Concrete material model

The expansion of corrosion products was modeled by a three-phase material model, which consisted of steel bar, corrosion products layer and concrete as shown in Figure 7. In this model, the corrosion products layer assumed with a constant thickness H of 1.0mm was modeled as an elastic material; their mechanical properties can be defined directly. The steel bar was also considered as elastic with a Young modulus of 200GPa.

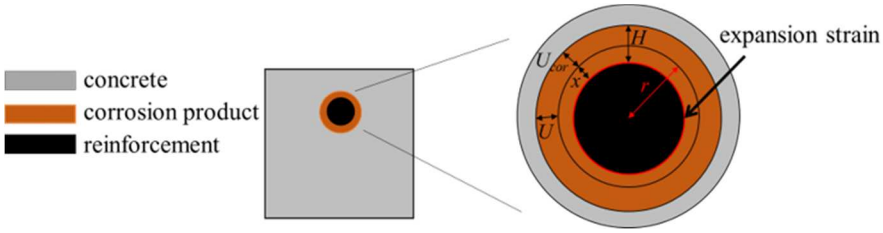

Figure 7: Corrosion expansion model

3.2 Truss Network model

The modeling of corrosion products movement was implemented using the Truss Network model[13]. The Truss Networks model with RBSM considering mass transportation into bulk concrete and through crack is first proposed by Nakamura[14]. The method has been applied by many researchers[15][16]. The mass transport problem governed by partial differential equations is usually simulated using a continuum model, while the RBSM is a discrete numerical approach. To tackle this problem the truss elements that connect each RBSM

particle are incorporated. These elements are generated by linking the center of each Voronoi particle and the intermediate points of the particle boundaries, which constitute the internal truss network as shown in Figure 8. To carry out the mass transport a simplified one-dimensional partial differential equation is applied to the internal truss network.

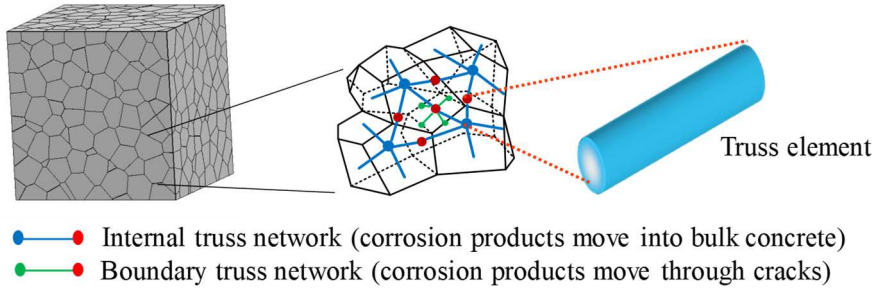

Figure 8: Truss Network model

It is well known that the mass transport process is faster in the presence of cracks. In order to consider this influence, another truss network is constructed on the particle boundaries referred to as the boundary truss network. The cross-section area of each boundary truss element is varied with the width of the potential crack generated on the corresponding boundary. Before cracking, the cross-section area is zero, and no mass transport is allowed at this stage. After cracking, the cross-section area is determined by multiplying the crack width with the edge length of the boundary, and mass can move through the opening crack.

The movement of corrosion products was described using the one-dimensional diffusion equation as follows:

$$\theta_w \frac{\partial R}{\partial t} = \frac{\partial}{\partial x}\left(\theta_w D_r \frac{\partial R}{\partial x}\right) \tag{2}$$

where R, D_r and θ_w are the concentration of corrosion products (g/mm^3), the diffusivity of the corrosion products (mm^2/s), and volume fraction of pore water (mm^3 of water / mm^3 of concrete), respectively. Commonly in the accelerated corrosion test the tested specimens are partly or completely immersed in salty water. Therefore, θ_w was assumed as a constant value of 0.1 in this study[9].

The internal truss elements were considered to carry the corrosion products into bulk concrete/pores and the diffusion coefficient D_r was assumed as 2.2×10^{-6}mm^2/s. When a crack wider than 0.01mm occurred, the corrosion products were allowed to move through the crack. The diffusion coefficient for the cracked part as well as the bulk concrete near the cracks was assumed as 2.2×10^{-2}mm^2/s. These values were decided by a parameter analysis, which is presented in the following section.

3.3 Coupling of cracking with corrosion products movement

The analysis of corrosion products movement using the Truss Network model was coupled with the analysis of corrosion cracking using the RBSM. Figure 9 shows the simulation flow of the proposed model. The input data were the time increment Δt and the applied current density i_c. Initially, the increment of mass loss Δm_i for a corroded rebar element i was decided using Faraday's law and the crack-dependent current efficiency N_i:

$$\Delta m_i = N_i i_c A_i \Delta t M/(nF) \quad (3)$$

where A_i is the outer face area of the corroded rebar element (mm^2), M is the molar mass of iron (55.85g/mol), n is the valency (2), and F is Faraday's constant (9.65×10^4C/mol). In the case of chloride-induced corrosion the corrosion distribution around a rebar is usually non-uniform[17]. Moreover, the corrosion is severer around the crack area, since the cracks can aggravate the ingress of chloride ions. The developed model accounted for such a behavior by adopting the local current efficiency, which varied with the crack width near a rebar element. The detail can be found in reference [18].

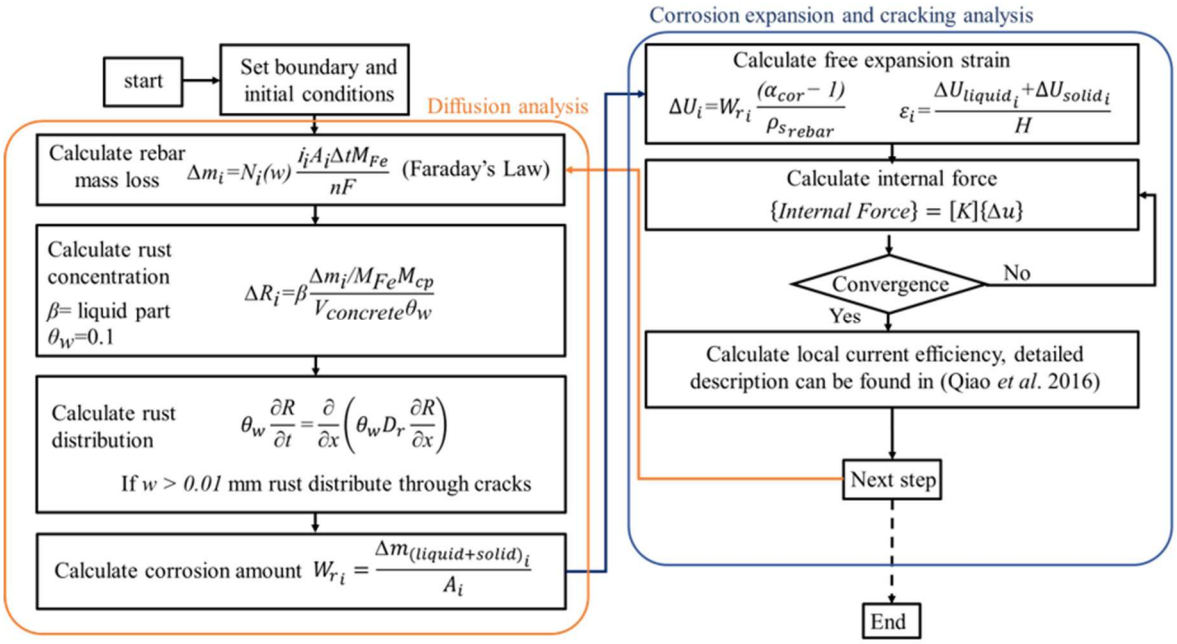

Figure 9: Simulation flow

On the other hand, as Gebreyouhannes and Maekawa[19] indicated the corrosion products consist of both solid and liquid phases. In the present model, only liquid phase was considered to take part in the moving process. Given a certain type of the corrosion products the concentration of the liquid phase was calculated with an assumed mass ratio β, which was added to the boundary between concrete and corrosion products layer as the initial condition for each incremental step. The liquid corrosion products were then distributed into bulk concrete and cracks through Truss Network. In addition, it was assumed that no corrosion products exuded from the concrete. Accordingly, on the concrete surface no-flux conditions were applied.

For the analysis of corrosion-induced cracking, the effective corrosion amount W_{ri} contributing to the expansion pressure was calculated considering both the solid phase and the remaining liquid phase at the boundary between concrete and corrosion products layer; The initial strains were calculated afterwards. In this study, the assumption of volume expansion α_{cor} followed Chen and Mahadevan[20] and Malumbela et al.[17]. They suggested that the corrosion products formed in accelerated corrosion tests are not stable. $Fe(OH)_2$ and $Fe(OH)_3$ having a volume expansion ratio in the range of 4.0 - 6.0 have been found to be dominant. In

our test, it was observed that the corrosion products were greenish-black in color, indicating large presence of $Fe(OH)_2$. Hence, the volume expansion α_{cor} was assumed as 4.0. The elastic modulus of the corrosion products was assumed to be 2.0GPa as obtained by Pease et al. [6]. After the cracking analysis, the local current efficiencies were updated based on the calculated crack widths for calculating the mass loss and initial strains for the next step.

3.4 Effect of Diffusion Parameters

The diffusivity of the corrosion products plays a great role in the cracking process. In this model, two different diffusion coefficients were used to consider the penetration of corrosion products into bulk concrete and the forming cracks separately. Figure 10 shows the effects of these two parameters on the surface crack development respectively. It was found that with an increase of the diffusion coefficient for bulk concrete a longer time was needed for crack initiation. On the other hand, a higher diffusion coefficient for the cracks may cause a slower cracking speed. Based on the analytical results, the diffusion coefficient for bulk concrete $D_{r(\text{pores})}$ was assumed as 2.2×10^{-6}mm^2/s and the one for the cracks $D_{r(\text{crack})}$ was assumed as 2.2×10^{-2}mm^2/s.

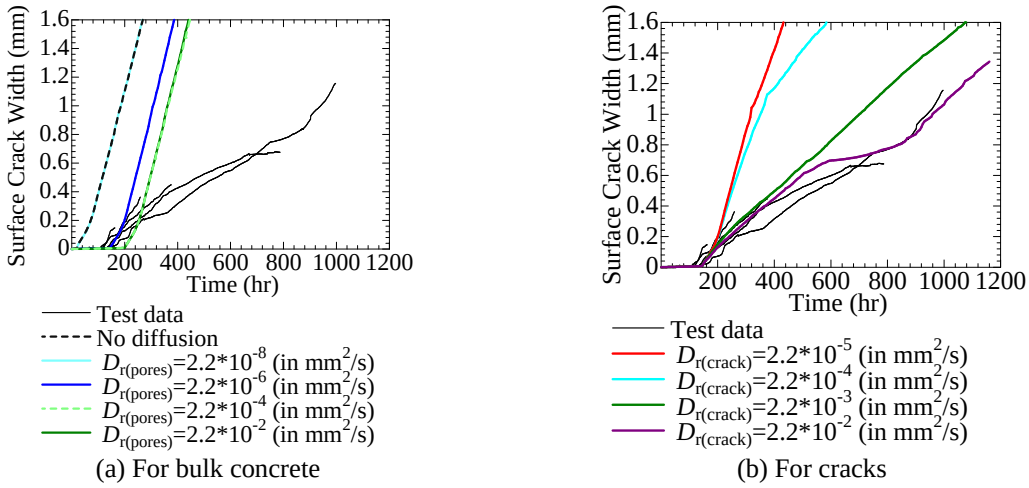

(a) For bulk concrete (b) For cracks

Figure 10: Effect of diffusion coefficients on surface crack development

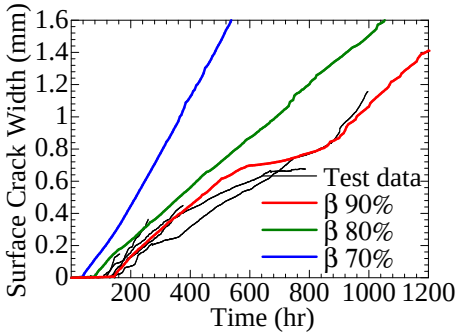

Figure 11: Effect of liquid percentage on surface crack development

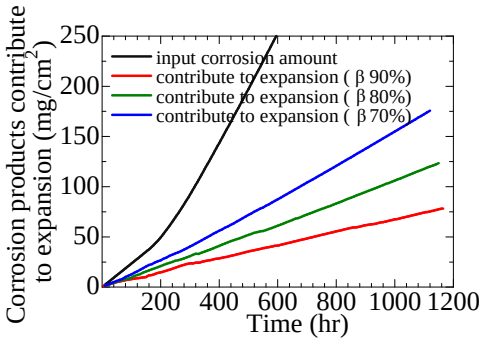

Figure 12: Proportion of corrosion products contributing to expansion

Another characteristic of the corrosion products included in this model was the solid and liquid phases, both of which had been considered to be important in the stress

development[3][19]. Figure 11 shows the effect of the liquid ratio β on the surface crack propagation. It shows that a higher percentage of the liquid phase may delay the crack initiation and result in a smaller cracking speed as well. The analytical results suggested a value of 90% for the electric corrosion test applied with a large current density of 900μA/cm^2. Figure 12 shows the development of the corrosion products that practically contributed to the expansion with various liquid ratios, 90%, 80% and 70%, respectively. These results confirmed that as the liquid ratio becomes smaller, more corrosion products can contribute to the expansion pressure, thus leading to a higher cracking speed as shown in Figure 12.

4 VALIDITY OF SIMULATION MODEL

The simulation method was further confirmed by comparing the simulation results with the test. An RBSM model with the same cross-section as that of the tested specimens was created as shown in Figure 13. Given that the length of the specimen may not influence the cracking behavior, it was reduced to 100 mm in the simulation to lessen the calculation burden. The model had a uniform mesh size of 5mm for the Voronoi particles.

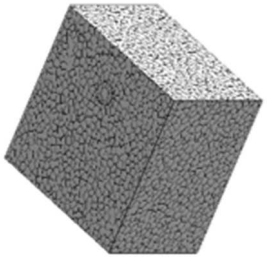

Figure 13: Simulation model

4.1 Crack Pattern, Corrosion Distribution, and Corrosion Products Movement

The internal crack patterns were examined for various corrosion amounts as shown in Figure 14. The cracks are plotted in different colors depending on the crack width. The yellow lines correspond to minor cracks, while the red lines represent the visible cracks wider than 0.13mm. For a small corrosion amount (<50mg/cm^2), minor cracks were found around the rebar. With an increase of corrosion amount, a visible crack started from the concrete surface and then propagated towards the rebar along with the appearance of two lateral cracks. This behavior is similar to that found in the test (see Figure 2), although the bottom crack could not be confirmed in the test for a rough examination by the naked eye.

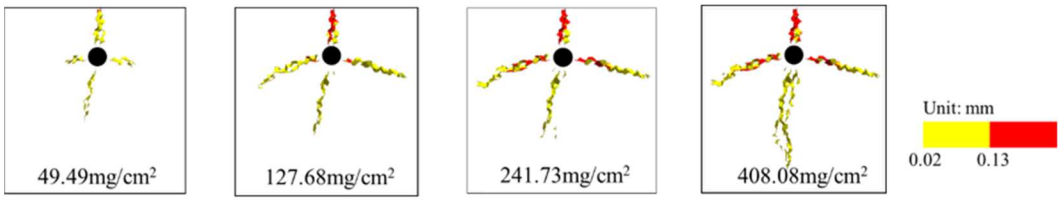

Figure 14: Simulated internal crack development

Figure 15 displays the movement of corrosion products. It is clear that the corrosion products were distributed gradually as the cracks developed. At the upper part of the rebar, the concentration of the corrosion products was higher, corresponding to a larger crack width

within this area. The simulation results suggested a progressive penetration of corrosion products into the lateral cracks and the neighboring bulk concrete.

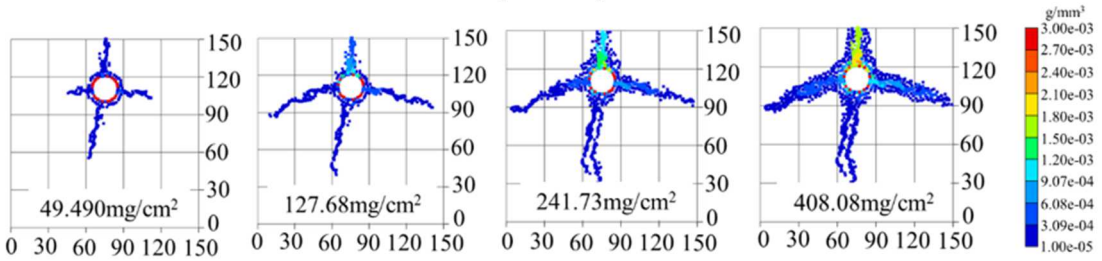

Figure 15: Distribution of corrosion products as corrosion develops

4.2 Surface Crack Development

The simulated surface crack propagation is compared with the experimental results as presented in Figure 16, showing a good agreement. The model developed in this study adopted several realistic values to describe the material properties of the corrosion products such as the volume expansion ratio and the elastic modulus, as opposed to those calibrated parameters used in the other studies[4][5]. This confirms that the movement of corrosion products has a great effect on the crack propagation, and a proper modeling of this movement is crucial to the prediction of the development of crack width.

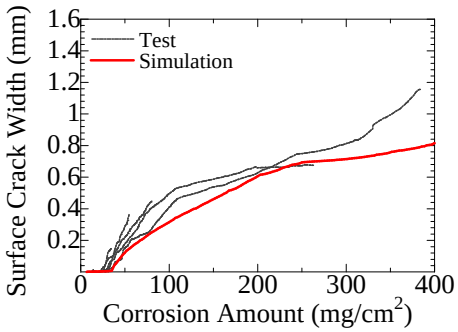

Figure 16: Simulated surface crack development

5 CONCLUSION

In this study, electric corrosion tests using single rebar specimens were carried out to investigate the evolution of corrosion-induced cracks. Following the test results, a numerical model based on three-dimensional RBSM coupled with Truss Network model was developed to simulate the concrete crack development considering the movement of corrosion products. The model was validated using the test results. The following conclusions can be derived:

- The development of surface crack width showed a two-stage bilinear process with decreasing cracking speed, corresponding to the penetration of corrosion products into the formed cracks.
- The model developed was able to reproduce the effect of corrosion products movement on the crack development and yielded accurate predictions of surface crack width.

Acknowledgement

This work was supported by Council for Science, Technology, and Innovation, “Cross-ministerial Strategic Innovation Promotion Program (SIP), Infrastructure Maintenance, Renovation, and Management” (funding agency: NEDO). The authors also acknowledge the supports of Grants-in-Aid for Scientific Research B (15H04033).

REFERENCES

[1] Maadawy, T. A. and Soudki, K. A.. “Effectiveness of impressed current technique to simulate corrosion of steel reinforcement in concrete. Journal Materials in Civil Engineering (2003), 15, 41-47.

[2] Michel, A. Pease, B. J. Peterová, A. Geiker, M. R. Stang, H. and Thybo, A. E. A.. “Penetration of corrosion products and corrosion-induced cracking in reinforced cementitious materials: experimental investigations and numerical simulations. Cement and Concrete Composites (2014), 47, 75-86.

[3] Zhao, Y. Dong, J. Wu, Y. and Jin, W. Corrosion-induced cracking model considering corrosion product-filled paste at the concrete/steel interface. Construction and Building Materials (2016)., 116, 273-280.

[4] Šavija, B. Luković, M. Pacheco, J. and Schlangen, E. Cracking of the concrete cover due to reinforcement corrosion: a two-dimensional lattice study. Construction Building Materials (2013), 44, 626-638.

[5] Sanz, B. Planas, J. and Sancho, J. M. A closer look to the mechanical behavior of the oxide layer in concrete reinforcement corrosion. International Journal of Solids and Structures (2015), 62, 256-268.

[6] Pease, B. J. Michel, A. Thybo, A. E. A. and Stang, H. Estimation of elastic modulus of reinforcement corrosion products using inverse analysis of digital image correlation measurements for input in corrosion-induced cracking model. In: the sixth International Conference on Bridge Maintenance, Safety and Management (IAMBAS) (2012).

[7] Šavija, B. Luković, M. Hosseini, S. A. S. Pacheco, J. and Schlangen, E. Corrosion induced cover cracking studied by X-ray computed tomography, nanoindentation, and energy dispersive X-ray spectrometry. Materials and Structures (2015), 48, 2043-2062.

[8] Tran, K. K. Nakamura, H. Kawamura, K. and Kunieda, M. Analysis of crack propagation due to rebar corrosion using RBSM. Cement and Concrete Composites (2011). 33, 906-917.

[9] Ožbolt, J. Oršanić, F. Balabanić, G. and Kušter, M. Modeling damage in concrete caused by corrosion of reinforcement: coupled 3D FE model. International Journal of Fracture (2012), 178, 233-244.

[10] Pedrosa, F. and Andrade, C. Corrosion induced cracking: effect of different corrosion rates on crack width evolution. Construction and Building Materials (2017), 133, 525-533.

[11] Yamamoto, Y. Nakamura, H. Kuroda, I. and Furuya, N. Analysis of compression failure of concrete by three-dimensional rigid body spring model. Journal of JSCE (2008), 64(4), 612-630 (in Japanese).

[12] Yamamoto, Y. Nakamura, H. Kuroda, I. and Furuya, N. Crack propagation analysis of reinforced concrete wall under cyclic loading using RBSM. European Journal of Environmental and Civil Engineering (2014), 18, 780-792.

[13] Nakamura, H., Srisoros, W., Yashiro, R. and Kunieda, M. Time-dependent structural analysis considering mass transfer to evaluate deterioration process of RC structures. Journal of Advanced Concrete Technology (2006), 4(1), 147-158.
[14] Nakamura, H. Srisoros, W. Kunieda, M and Tanabe, T. Time Dependent Structural Analysis Considering Mass Transfer, The Seventh International Conference on creep, shrinkage and durability of concrete and concrete structure (CONCREEP7) (2005), Nantes, France, pp. 151-162.
[15] Wang, L., Soda, M., and Ueda, T. Simulation of chloride diffusivity for cracked concrete based on RBSM and truss network model. Journal of Advanced Concrete Technology (2007), 6(1), 143-145.
[16] Grassl, P. A lattice approach to model flow in cracked concrete. Cement and Concrete Composite (2009), 31, 454-460.
[17] Malumbela, G., Moyo, P. and Alexander, M. A step towards standardizing accelerated corrosion tests on laboratory reinforced concrete specimens. Journal of South African Institution of Civil Engineering (2012), 54, 78-85.
[18] Qiao, D. Nakamura, H. Yamamoto, Y. and Miura, T. Modelling of corrosion-induced damage in reinforced concrete considering electro-mechanical coupling. Journal of Advanced Concrete Technology (2016), 14, 664-678.
[19] Gebreyouhannes, E. and Maekawa, K. “Nonlinear gel migration in cracked concrete and broken symmetry of corrosion profiles. Journal of Advanced Concrete Technology (2016), 14, 271-266.
[20] Chen, D. and Mahadevan, S. Chloride-induced reinforcement corrosion and concrete cracking simulation. Cement and Concrete Composite (2008), 30, 227-238.